

CBPF-NF-032/82  
CALCULATIONS OF HYPERFINE INTERACTIONS IN  
TRANSITION METAL COMPOUNDS IN THE LOCAL  
DENSITY APPROXIMATION

by

Diana Guenzburger

CENTRO BRASILEIRO DE PESQUISAS FÍSICAS - CBPF/CNPq  
Rua Xavier Sigaud, 150  
22290 Rio de Janeiro, RJ - BRASIL

CALCULATIONS OF HYPERFINE INTERACTIONS IN TRANSITION METAL  
COMPOUNDS IN THE LOCAL DENSITY APPROXIMATION

Diana Guenzburger

Centro Brasileiro de Pesquisas Físicas - CBPF/CNPq  
Rua Xavier Sigaud, 150  
22290 Rio de Janeiro, RJ, BRASIL

## ABSTRACT

A survey is made of some theoretical calculations of electrostatic and magnetic hyperfine interactions in transition metal compounds and complex ions. The molecular orbital methods considered are the Multiple Scattering and Discrete Variational, in which the local  $X\alpha$  approximation for the exchange interaction is employed. Emphasis is given to the qualitative informations, derived from the calculations, relating the hyperfine parameters to characteristics of the chemical bonds.

## I. INTRODUCTION

Hyperfine interactions are electromagnetic interactions between a nucleus and surrounding charges, other than the Coulomb interaction between the external charge distribution, and the nucleus considered as a point charge. These small interactions are of the order of  $10^{-8}$  eV, and may be detected through their effect on the nuclear or electronic energy levels.

The experimental techniques employed to measure hyperfine interactions are, most commonly, spectroscopic in nature. Some techniques that involve only the ground state of the nucleus are Nuclear Magnetic Resonance<sup>(1)</sup>, Electron Paramagnetic Resonance<sup>(2)</sup>, Nuclear Quadrupole Resonance<sup>(3)</sup> etc. Other techniques, such as Mössbauer spectroscopy<sup>(4)</sup> and Perturbed Angular Correlation<sup>(5)</sup>, involve nuclear excited states as well.

Hyperfine interactions provide information on the nucleus, and on its electronic environment. As such, they have become an important tool in the investigation of solid state electronic properties, and in the description of chemical bonds in molecules.

Investigations of electronic properties through hyperfine interactions have outstanding importance for transition metal compounds and complex ions. Many such compounds have unpaired electrons in open shells and are suitable for Electron Paramagnetic Resonance studies. Others, due to the characteristics of the metal nuclei, are convenient probes for Mössbauer spectroscopy studies. Among these last, Fe has been extensively employed,

through the 14.4 keV transition of  $^{57}\text{Fe}$ , providing wealthy data which can be related to ionic or covalent bonding to ligands.

In relating experimental measurements to electronic properties, wave functions of good quality are needed to calculate the hyperfine parameters. On the other hand, wave functions of full Hartree-Fock level are still difficult to obtain for transition metal compounds. The Hartree-Fock-Slater method<sup>(6)</sup>, which employs the local density approximation known as  $X\alpha$  for the exchange interaction, constitutes an alternative which is less costly computationally. The success achieved with this method in calculating other properties of transition metal molecules has encouraged its use in hyperfine interactions studies, and now a sufficient number of investigations have been reported to allow an assessment of some of its successes and failures.

## II. ELECTROSTATIC HYPERFINE INTERACTIONS

The energy of the electrostatic interaction of a nuclear charge distribution  $\rho(\vec{r})$  placed in a potential  $\phi(\vec{r})$  due to external charges is:

$$W = \int \rho(\vec{r}) \phi(\vec{r}) d\tau \quad (1)$$

Expanding  $\phi(\vec{r})$  in a Taylor series around  $\vec{r} = 0$ , and defining the total nuclear charge as  $Ze = \int \rho(\vec{r}) d\tau$ , we obtain:

$$W = Ze \phi(0) + \sum_{\alpha=1}^3 \left( \frac{\partial \phi}{\partial x_{\alpha}} \right)_0 \int \rho(\vec{r}) x_{\alpha} d\tau + \frac{1}{2} \sum_{\alpha} \sum_{\beta} \left( \frac{\partial^2 \phi}{\partial x_{\alpha} \partial x_{\beta}} \right)_0 \int \rho(\vec{r}) x_{\alpha} x_{\beta} d\tau + \dots \quad (2)$$

The first term is the Coulomb point charge interaction, and the second (dipole) term vanishes because of parity conservation of the nuclei. Rewriting the third term by introducing  $r^2 = \sum_{\alpha} x_{\alpha}^2$ , we find:

$$W' = \frac{1}{6} \sum_{\alpha} \left( \frac{\partial^2 \phi}{\partial x_{\alpha}^2} \right)_0 \int \rho(\vec{r}) r^2 d\tau + \frac{1}{6} \sum_{\alpha} \sum_{\beta} \left( \frac{\partial^2 \phi}{\partial x_{\alpha} \partial x_{\beta}} \right)_0 \int \rho(\vec{r}) (3x_{\alpha} x_{\beta} - r^2 \delta_{\alpha\beta}) d\tau \quad (3)$$

From the first term in  $W'$  is derived the monopole shift  $\delta$  of a nuclear level. Making use of Poisson's equation  $\nabla^2 \phi(\vec{r}) = -4\pi \rho_{e\ell}(\vec{r})$  at  $\vec{r} = 0$ , we find:

$$\delta = \frac{2\pi}{3} Ze^2 |\Psi(0)|^2 \langle r^2 \rangle_N \quad (4)$$

where  $\rho_{e\ell} \equiv -e |\Psi(0)|^2$  is the electronic charge density within the nuclear volume and  $\langle r^2 \rangle_N$  is the mean square radius of the nuclear charge distribution.

In a nuclear resonance (Mössbauer) experiment, if  $\rho_{e\ell}(0)$  is different at the emitting (S) and absorbing (A) nuclei, because of different electronic environments, an isomer shift (IS)<sup>(7)</sup> of the resonance line is observed, given by:

$$IS = \frac{2\pi}{3} Ze^2 [\langle r^2 \rangle_e - \langle r^2 \rangle_g] [|\Psi(0)|_A^2 - |\Psi(0)|_S^2] S'(Z) \quad (5)$$

where  $\langle r^2 \rangle_e$  and  $\langle r^2 \rangle_g$  are the mean square nuclear radii in the excited and ground nuclear levels of the Mössbauer transition, and  $S'(Z)$  a factor to account for relativistic effects.

The second term of  $W'$  in Eq.(3) expresses classically the interaction between the electric field gradient tensor and the nuclear quadrupole moment tensor<sup>(8)</sup>. The quantum mechanical treat-

ment of this interaction involves the evaluation of the matrix elements of the electrostatic Hamiltonian  $H_{e\ell}$  defined as:

$$H_{e\ell} = \sum_{i=1}^N \sum_{p=1}^Z \frac{eK_i}{|\vec{r}_i - \vec{r}_p|} \quad (6)$$

where  $\vec{r}_p$  are the position vectors of the Z nuclear protons surrounded by N exterior charges  $K_i$ . Expanding  $(1/|\vec{r}_i - \vec{r}_p|)$  in Legendre polynomials and making use of the addition theorem of the spherical harmonics, we find:

$$H_{e\ell} = \sum_{\ell, m} \left[ \sum_p \sqrt{\frac{4\pi}{2\ell+1}} e r_p^\ell Y_\ell^m(\theta_p, \phi_p) \right] \left[ \sum_i \sqrt{\frac{4\pi}{2\ell+1}} \frac{K_i Y_\ell^{m*}(\theta_i, \phi_i)}{r_i^{\ell+1}} \right]$$

or

$$H_{e\ell} = \sum_{\ell, m} [\epsilon_{\ell m}] [v_{\ell m}^*] \quad (7)$$

The quadrupolar Hamiltonian  $H_Q$  is the  $\ell=2$  term of the expansion. This interaction may be considered as a perturbation that will mix the substates of a nuclear level of spin I. Making use of the Wigner-Eckart theorem and the definition of the nuclear quadrupole moment Q,

$$Q = \langle II | \sum_p (3z_p^2 - r_p^2) | II \rangle \quad (8)$$

the matrix elements of  $H_Q$  are expressed as

$$\langle Im_j | H_Q | Im_i \rangle = \frac{eQ}{2} \frac{\langle I2m_i m | Im_j \rangle}{\langle I210 | II \rangle} v_{2m}^* \quad (9)$$

where  $m_j$  and  $m_i$  are projections of the nuclear spin  $I$  on the  $z$ -axis and the coefficient on the right side includes Clebsch-Gordon coefficients, with the usual selection rule  $m = m_j - m_i$ . The electric field gradient tensor obtained from the field at the nucleus due to the external charges  $K_i$  has as its components:

$$V_{k\ell} = \left\{ \frac{\partial^2}{\partial x_k \partial x_\ell} \left[ \sum_i \frac{K_i}{|\vec{r}_i - \vec{r}_n|} \right] \right\}_{\vec{r}_n \rightarrow 0} = \sum_i K_i \frac{3x_{ik}x_{i\ell} - \delta_{k\ell}r_i^2}{r_i^5} \quad (10)$$

The matrix representing this tensor is symmetric and, due to Laplace's equation, traceless, so that only five independent components remain. These may be related to the elements  $v_{2m}$  by a simple transformation of coordinates. In a coordinate system in which  $V_{k\ell}$  is diagonal, we have then:

$$\begin{aligned} v_{20} &= V_{zz}/2 \\ v_{2\pm 1} &= 0 \\ v_{2\pm 2} &= \frac{1}{2\sqrt{6}} (V_{xx} - V_{yy}) \end{aligned} \quad (11)$$

Two special cases may be considered. In the first case, the charge distribution around the nucleus has axial symmetry, and the quadrupole interaction (Eq.(9)) becomes simply:

$$E_Q = \langle IM | H_Q | IM \rangle = eQ \left[ \frac{3M^2 - I(I+1)}{4I(2I-1)} \right] V_{zz} \quad (12)$$

In the second case,  $I = 3/2$  and the matrix with elements defined by Eq.(9) may be diagonalized to give two doubly degenerate levels corresponding to  $|M| = 3/2$  and  $|M| = 1/2$ . The splitting of a  $I = 3/2$  level is seen, for example, in Mössbauer experiments of



Fe, Ru and Au isotopes, of which many compounds have been investigated.

Defining further:

$$\eta = \frac{V_{xx} - V_{yy}}{V_{zz}} \quad (13)$$

with the convention that  $|V_{zz}| \geq |V_{yy}| \geq |V_{xx}|$ , so that  $0 \leq \eta \leq 1$ , we have finally:

$$\Delta EQ = -\frac{eQ}{2} V_{zz} \left(1 + \frac{\eta^2}{3}\right)^{1/2} \quad (14)$$

which is the energy splitting of the two sublevels  $|M| = 3/2$  and  $|M| = 1/2$ . In a Mössbauer experiment, this is manifested by a splitting of the resonance line. In the case of axial symmetry, Eq.(14) reduces to:

$$\Delta EQ = -\frac{eQ}{2} V_{zz} \quad (15)$$

For higher spin states, the matrix  $\langle H_Q \rangle$  may be diagonalized; for  $I < 1$ , no splitting occurs.

### III. MAGNETIC HYPERFINE INTERACTIONS

The magnetic moment of a nucleus  $\vec{u}$  interacts with an external magnetic field, which, when arising from the surrounding electrons, is called the hyperfine field<sup>(2)</sup>. We have then, for the magnetic dipole interaction Hamiltonian:

$$\mathcal{H}_{HF} = -\vec{u} \cdot \vec{H} = -g_N \mu_N \vec{I} \cdot \vec{H} \quad (16)$$

where  $g_N$  and  $\mu_N$  are, respectively, the nuclear g factor and nuclear magneton.

The calculation of magnetic hyperfine interactions consists in evaluating the first order correction on the energy levels of the system considered

$$E_{\text{HF}} = \langle \Psi | \mathcal{H}_{\text{HF}} | \Psi \rangle \quad (17)$$

with the hyperfine Hamiltonian defined as

$$\mathcal{H}_{\text{HF}} = \sum_i (\mathcal{H}_{\text{F}}^i + \mathcal{H}_{\text{D}}^i + \mathcal{H}_{\text{L}}^i)$$

where

$$\begin{aligned} \mathcal{H}_{\text{F}}^i &= \frac{8\pi}{3} g_e g_N \mu_B \mu_N \delta(\vec{r}_i) \vec{I} \cdot \vec{S}_i \\ \mathcal{H}_{\text{D}}^i &= g_e g_N \mu_B \mu_N \left[ 3 \frac{(\vec{I} \cdot \vec{r}_i)(\vec{S}_i \cdot \vec{r}_i)}{r_i^5} - \frac{\vec{I} \cdot \vec{S}_i}{r_i^3} \right] \\ \mathcal{H}_{\text{L}}^i &= g_e g_N \mu_B \mu_N \frac{\vec{I} \cdot \vec{L}_i}{r_i^3} \end{aligned} \quad (18)$$

In Eqs. (18),  $g_e$  is the electron g factor and  $\mu_B$  the Bohr magneton.  $\mathcal{H}_{\text{F}}$  is the Fermi (contact) interaction,  $\mathcal{H}_{\text{D}}$  the spin dipolar and  $\mathcal{H}_{\text{L}}$  the orbital dipolar interactions. This last, in many cases, may be considered negligible.

To establish a link with experimental measurements, a spin Hamiltonian is defined, which allows the description of experiment

tal results through a limited number of parameters (the "hyperfine constants"). For this purpose, Eqs. (18) are used to accomplish the integration in Eq. (17) over the electronic spatial coordinates leaving the nuclear and electronic spin operators in their explicit form.

We have then, for the Fermi interaction

$$\mathcal{H}_F = a \vec{I} \cdot \vec{S}$$

where  $a = \frac{8\pi}{3} g_e g_N \mu_B \mu_N \sum_i n_i |\psi_{i\uparrow}(0)|^2$  for the direct interaction of unpaired s-symmetry electrons with the nucleus, or

$$a = \frac{8\pi}{3} g_e g_N \mu_B \mu_N \sum_i n_i \left[ |\psi_{i\uparrow}(0)|^2 - |\psi_{i\downarrow}(0)|^2 \right] \quad (19)$$

for the interaction of the spin density at the nucleus which arises through the polarization of s-symmetry electrons in closed shells by unpaired electrons of different symmetry<sup>(9)</sup>.

The spin dipolar interaction may be expressed in terms of a symmetric and traceless tensor  $\vec{B}$ , such that

$$\mathcal{H}_D = \vec{I} \cdot \vec{B} \cdot \vec{S}$$

The diagonal components of the tensor  $\vec{B}$  may be expressed in terms of the parameters:

$$\begin{aligned} b &= \frac{1}{2} g_e g_N \mu_B \mu_N \sum_i n_i \int \psi_i^*(\vec{r}) \left[ \frac{3z^2 - r^2}{r^5} \right] \psi_i(\vec{r}) d\tau \\ b' &= \frac{3}{2} g_e g_N \mu_B \mu_N \sum_i n_i \int \psi_i^*(\vec{r}) \left[ \frac{x^2 - y^2}{r^5} \right] \psi_i(\vec{r}) d\tau \end{aligned} \quad (20)$$

The summations in Eqs. (20) include all unpaired electrons of appropriate symmetry, as well as polarized electrons in closed shells; in cases of axial symmetry,  $b'$  is equal to zero.

In a Mössbauer experiment the magnetic hyperfine interaction is seen to lift the degeneracy of the  $|IM\rangle$  nuclear levels.

#### IV. CALCULATIONS OF HYPERFINE INTERACTIONS

The Hartree-Fock-Slater<sup>(6)</sup> approximation for the calculation of molecular orbitals  $\psi_i$  of transition metal compounds and complexes is based on the local approximation for the exchange potential, expressed as (in Hartrees):

$$V_{x\alpha\uparrow}(\vec{r}) = -3\alpha \left[ \frac{3}{4\pi} \sum_i n_i |\psi_{i\uparrow}(\vec{r})|^2 \right]^{1/3} \quad (21)$$

with a similar expression for spin down. The parameter  $\alpha$ , as derived rigorously from a variational treatment<sup>(10)</sup>, is equal to  $2/3$ . However, different values have been used, as derived by fitting the total energies obtained for free atoms to the Hartree-Fock energies<sup>(6)</sup>.

In this approximation, the one - electron equations to be solved are of the form

$$\left[ -\frac{1}{2} \nabla^2 + V_c(\vec{r}) + V_{x\alpha\uparrow}(\vec{r}) \right] \psi_{i\uparrow}(\vec{r}) = \epsilon_i \psi_{i\uparrow}(\vec{r}) \quad (22)$$

where  $V_c(\vec{r})$  is the Coulomb potential due to both electrons and nuclei.

The methods of calculation which have been employed are the Multiple Scattering (MSX $\alpha$ )<sup>(11)</sup> and Discrete Variational (DVM)<sup>(12)</sup>. The description of these methods will not be given here, since this has been done in detail in the original literature. It will be sufficient to remind that in the MSX $\alpha$ , a "muffin-tin" approximation to the potential is employed, with spheres around each nucleus defining regions of spherically - symmetrical potentials. In these regions, the wave functions are then an expansion of spherical harmonics multiplied by a numerical radial function, this last being quite flexible to adapt to the molecular potential. In the DVM method no such approximation to the potential is made, and the molecular orbitals are expanded in a basis of atomic orbitals; numerical integrations are performed to calculate the matrix elements of the secular equations.

#### IV.a ISOMER SHIFTS

The problem posed in the calculation of isomer shifts as in Eq.(5) is the evaluation of the electronic densities at the nuclei. In the orbital approximation, we have then:

$$IS = \alpha \left[ \sum_i n_i |\psi_i(0)|_A^2 - \sum_j n_j |\psi_j(0)|_S^2 \right] \quad (22)$$

where the summations are over the molecular orbitals of s-type symmetry. Since the early days of Mössbauer spectroscopy, many attempts have been made to evaluate the so-called calibration constant  $\alpha$  of  $^{57}\text{Fe}$ , in order to obtain the value of the nuclear parameter  $\Delta \langle r^2 \rangle_{e,g}$ . For this purpose, Hartree-Fock wave functions of free ions were related to the IS values of ionic compounds. Besides this quantitative interest, questions arise as to what

bonding mechanisms the different values of IS of different Fe compounds were to be ascribed. The main effects that seemed relevant were the screening of 3s and 4s electrons by 3d electrons, differences in the number of 4s electrons in different configurations, and Fe orbital contractions when orthogonality to ligand orbitals was considered ("overlap distortion"). But no answer could be given as to the relative roles of these effects in an actual molecule.

Walsh and Ellis<sup>(13)</sup> studied the variations of the electron density at the nucleus of the  $\text{FeAr}_{12}$  cluster to study the IS of  $^{57}\text{Fe}$  in a solid argon matrix. The DVM method was used, but the potential was not made self-consistent. With these calculations it was shown that overlap distortion and potential distortion (relaxation) have opposite effects on the electronic density at the nucleus, and partially cancel.

The first attempts to study  $^{57}\text{Fe}$  isomer shifts in complexes with the  $\text{MSX}\alpha$  method were quite discouraging. Ellis and Averill<sup>(14)</sup> investigated the tetrahedral anions  $[\text{FeCl}_4]^{-1}$  and  $[\text{FeCl}_4]^{-2}$  in the spin-restricted approximation, and obtained a calibration constant  $\alpha \sim -0.8$ , very far from the range of "reasonable" values which had been obtained from free-ion calculations. A detailed study of the IS of several high-spin halogen compounds of Fe was made with the  $\text{MSX}\alpha$  method by de Siqueira et al.<sup>(15)</sup> Both octahedral and tetrahedral clusters were considered in spin-unrestricted calculations. This work showed that electron densities at the Fe nucleus were dependent on the radii chosen in forming the "muffin-tin" model potential, and so no definite value of the calibration con-

stant could be derived.

The subsequent continuation of this work to include covalent complexes of Fe, has, however, changed this outlook to a certain extent. Complexes of  $\text{Fe}^{+2}$  and  $\text{Fe}^{+3}$  with  $\text{CN}^-$  ligands have a much more covalent character than halogen complexes, and this is made evident by their low-spin configurations. The octahedral complexes  $[\text{Fe}(\text{CN})_6]^{-4}$  and  $[\text{Fe}(\text{CN})_6]^{-3}$  were studied with the  $\text{MSX}\alpha$  method and values of  $|\psi(0)|^2$  derived<sup>(16)(17)</sup>. The tetrahedral ferrate ion  $\text{FeO}_4^{-2}$ , in which Fe has the unusual formal charge +6, is present in compounds having the lowest values of isomer shifts of all Fe compounds measured. This ion, which is in a  $^3A_2$  ground state, with two electrons in the last occupied e orbital, was investigated with the spin-polarized  $\text{MSX}\alpha$  method<sup>(18)</sup>.

A compilation of these results is given in table I and figure I. Although the dependence on the chosen "muffin-tin" scheme is evident, this model does provide useful information, if reasonable empirical criteria are used in defining the model potential. For example, in the case of the  $\text{CN}^-$  complexes, the choice of the "muffin-tin" tangent spheres radii was very limited, due to the short C-N distance, which allowed only small radii associated to the C and N atoms. One may also make use of Pauling's ionic or covalent radii to help in defining a "muffin-tin" potential.

In table I and figure I, some trends in  $|\psi(0)|^2$  may be observed. The values of  $|\psi(0)|^2$  for the 1s and 2s orbitals have not been considered because they show differences among different compounds which are very small. For the Fe(3s) and valence or-

bitals, the fluorides show an increase in the electron density at the origin with an increase in the Fe formal oxidation state. The increase in the valence density (Fe(4s)) plays an important role in this trend. As for  $[\text{Fe}(\text{CN})_6]^{-4}$  and  $[\text{Fe}(\text{CN})_6]^{-3}$ , one may explain the considerably lower values of the isomer shifts, compared to the high-spin (ionic) complexes of same formal charge on Fe, by the much larger valence (Fe(4s)) density at the origin present in the covalent ions, as a result of the strong  $\sigma$ -donation property of the  $\text{CN}^-$  ligands.

Besides increase in 4s charge densities, another mechanism which has been evoked to explain differences in IS values are changes in 3d populations, which would result in differences in 3s densities at the origin, since the 3d electrons screen the 3s electrons from the nucleus. Examination of table I shows small differences in  $|\psi(0)|_{3s}^2$ , and so this mechanism is seen to be less important.

Populations of an atom in a molecule may be approximately defined in the MSX $\alpha$  model by considering the amplitude of the radial functions inside the atomic sphere, as compared to the free atom<sup>(17)(19)</sup>. Comparison of the Fe(3d) populations, calculated in this manner for the covalent complexes in table I, show small differences, which is consistent with the small differences in  $|\psi(0)|_{3s}^2$ . Particularly striking is the case of  $\text{FeO}_4^{-2}$ : formally, Fe has a 3d<sup>2</sup> configuration, but in the molecule the 3d population increases to 5.8<sup>(18)</sup>. The very low IS value may thus be ascribed mainly to a large "invasion" of valence electrons, caused by the very attractive potential of  $\text{Fe}^{+6}$ : the population analysis results in  $\sim 1.3$  Fe(4s) electrons.



One must bear in mind, however, that Coulomb correlation is not included in this approximation; if it were considered, these results might change somewhat, in that correlation would tend to oppose the accumulation of electronic charge, especially in orbitals of limited spacial extent, such as Fe(3d).

In figure I, the IS and electron densities are related by a straight line, which gives the value  $\alpha = -0.29$  for the IS calibration constant, similar to the value  $\alpha = -0.30$  obtained from Hartree-Fock "ad-initio" calculations of  $\text{CN}^-$  and  $\text{F}^-$  complexes<sup>(20)</sup>. Although the present number must be viewed with caution, the results do indicate that a consistent trend among different Fe compounds is obtained.

The development of low-temperature matrix isolation techniques has made possible the measurement of hyperfine interactions in isolated molecules and clusters of transition elements. Since the inert-gas matrixes are expected to interact very little with the clusters, it is an ideal situation to study chemical bonds without exterior interference. Hyperfine parameters have been calculated with the  $X\alpha$ -DVM method for  $\text{Fe}_2$  and other Fe dimers, namely FeMn, FeCo, FeNi and FeCu, and related to  $^{57}\text{Fe}$  Mössbauer measurements in noble gas matrixes<sup>(21)</sup>. This task met with several difficulties. These molecules present a dense band of valence one-electron levels, and assigning the ground-state configuration based solely on the molecular orbital levels schemes is not possible. In these circumstances, Coulomb correlation effects are also expected to be important, and Configuration Interaction calculations would be required. However, certain general informations

on the electronic densities at the Fe nucleus were obtained. For example, it is observed that the sum of the contributions  $|\psi_i(0)|^2$  of the valence orbitals, if occupied by the same number of electrons, decreases slightly when going from FeMn to FeCu. This is related to an increase in the Fe(3d) Mulliken population and decrease in 4s. It is curious to notice that this same trend may explain the increase of the IS values of Fe impurities in transition metal hosts Mn to Cu, as well as those of first-neighbour Fe atoms in Fe metal containing Mn, Co, Ni and Cu impurities<sup>(21)</sup>. This suggests that isomer shifts of systems involving transition elements metallic bonds depend on fundamental features that may be represented by a single bond between two atoms.

In the case of Fe<sub>2</sub>, the effect of different interatomic distances on  $|\Psi(0)|^2$  was also investigated. The results are shown in figure II. There is a dramatic increase of  $|\Psi(0)|^2$  at shorter distances, not followed by any significant changes in 3d or 4s populations. This may be interpreted in terms of an orthogonality ("overlap distortion") effect, which, with the LCAO basis used in the DVM method, is manifested by a greater participation of the inner atomic orbitals of the basis (mainly 3s) in the valence molecular orbitals. Again, the trend shown in figure II may be related to the trend observed for isomer shifts of Fe metal at different pressures<sup>(21)</sup>: at higher pressures, the isomer shifts are smaller.

Another interesting research area in Fe compounds is the investigation, in inert matrixes, of molecules that undergo photochemical reactions. The photochemical decomposition of Fe(CO)<sub>5</sub>

is known to produce species in which one or more CO ligands have been detached. Molecular orbital calculations of the fragments  $\text{Fe}(\text{CO})_n$ ,  $5 \geq n \geq 1$ , have been performed recently with the DVM method, in the spin-unrestricted form for the case of open-shell fragments<sup>(22)</sup>. Hyperfine interactions were studied and related to bonding characteristics. For the case of  $\text{Fe}(\text{CO})_5$  and  $\text{Fe}(\text{CO})_4$ , the IS values are known: for  $\text{Fe}(\text{CO})_4$ , the quadrupole splittings  $\Delta E_Q$  and IS values were measured in recent experiments of Mössbauer spectroscopy of  $\text{Fe}(\text{CO})_5$  absorbed in a polyethylene film at room temperature, and irradiated with UV light<sup>(23)</sup> (see table II).

The calculated values of  $|\Psi(0)|^2$  for iron pentacarbonyl and its fragments are very similar, and so similar IS values are predicted. As the number of carbonyls decreases, a small decrease in  $|\Psi(0)|^2$  is observed; for the smaller fragments  $\text{Fe}(\text{CO})_2$  and  $\text{FeCO}$ , the trend is reversed. This is explained as follows: in  $\text{Fe}(\text{CO})_5$ , a large valence contribution to  $|\Psi(0)|^2$  is calculated. This is not due to a large Fe(4s) population, since this is quite negligible (see table II), but to participation of the Fe(3s) orbitals of the basis in the valence molecular orbitals ("contraction"). This "contraction" is decreased slightly in  $\text{Fe}(\text{CO})_4$ , resulting in a slightly smaller  $|\Psi(0)|^2$  and, accordingly, higher value of the IS (see table II). This result shows that, in this case, an analysis based solely on the 3d and 4s populations would be misleading, as seen in table II. As the number of CO ligands decrease further, an increase in Fe(4s) populations is observed, and this compensates for the smaller "contraction" of valence orbitals.

In concluding this section, it would be worthwhile to mention

that little systematic investigation has been done to evaluate the effect of the local exchange approximation on the sensitive hyperfine parameters. Comparisons of  $|\psi(0)|^2$ , calculated in the  $X\alpha$  approximation, with Hartree-Fock values, were made for Ru atoms and ions, in several configurations<sup>(24)</sup>. Several values of  $\alpha$  were investigated, since, as mentioned before, not always the value  $\alpha = 2/3$  is employed. Similar studies for other elements would certainly be useful.

#### IV.b. QUADRUPOLE INTERACTION

The electronic contributions to the electric field gradient that originates the quadrupole splitting  $\Delta EQ$  of a nuclear level with spin  $I = 3/2$ , as in Eq. (14), are given by:

$$V_{zz} = -e \sum_i n_i \langle \psi_i | \frac{3\cos^2\theta - 1}{r^3} | \psi_i \rangle \quad (23)$$

$$\frac{V_{xx} - V_{yy}}{e} = \sum_i n_i \langle \psi_i | \frac{3\sin^2\theta \cos 2\phi}{r^3} | \psi_i \rangle$$

where  $\psi_i$  are molecular orbitals.

Considerable less attention has been given to the theoretical study of quadrupole splittings in transition metal compounds with  $X\alpha$  methods, as compared to isomer shifts. Early  $MSX\alpha$  calculations<sup>(14)</sup> of tetrahedral  $FeCl_4^{-1}$  and  $FeCl_4^{-2}$  allowed the comparison of  $\langle r^{-3} \rangle$  values of 3d-like orbitals with atomic and ionic values. More recently, the  $MSX\alpha$  method has been applied<sup>(25)</sup> in the overlapping-spheres version, to calculate  $\Delta EQ$  values in the very covalent complexes  $[Fe(CN)_5NO]^{-2}$ ,  $[Fe(CN)_5CO]^{-3}$ , and

$[\text{Fe}(\text{CN})_5\text{N}_2]^{-3}$ . Special attention was given to analyse the relative roles of  $\sigma$  and  $\Pi$  bonding of the various ligands in producing the field gradients. For calculating  $\Delta\text{EQ}$ , an atomic model was employed, using the Fe 3d and 4p populations obtained in the molecular calculations. The agreement with the experimental values was found to be good.

The  $X\alpha$ -DVM method was recently employed<sup>(26)</sup> to calculate quadrupole splittings of linear Au(I) compounds, for which experimental values were available from  $^{197}\text{Au}$  Mössbauer spectroscopy. Special numerical integration schemes were employed, both for the DVM variational calculation as for the calculation of the matrix elements of Eq.(23). These last were fully evaluated, including multicenter terms and core orbitals. Fairly good agreement with experimental values was found for  $[\text{Au}(\text{CN})_2]^{-1}$  and  $[\text{AuCl}_2]^{-1}$ . The large negative value of  $\Delta\text{EQ}$  measured for  $\text{K}[\text{Au}(\text{CN})_2]$  was seen to derive mainly from large one-center contributions given by  $\sigma_{\mu}^+$  valence orbitals with significant core atomic orbital (Au(5p)) character or, in other words, contracted towards the Au atom in the molecular axis direction. The inclusion of the core 5p orbital in the LCAO expansion greatly magnifies the electric field gradient of a  $\sigma_{\mu}^+$  orbital, due to the large  $\langle r^{-3} \rangle_{5p}$  value.

Finally, it may be mentioned that the effect of the  $X\alpha$  local density approximation on  $\langle r^{-3} \rangle$  values of ions and atoms, as compared to Hartree-Fock values, was studied for two transition elements<sup>(24)</sup>, namely Fe and Ir, in several configurations and several values of  $\alpha$ . The best agreement is found for  $\alpha = 2/3$ ; the

d and f orbitals compare better with the Hartree-Fock values than the p orbitals, the larger discrepancies being observed for the outer p orbitals.

#### IV.c. MAGNETIC HYPERFINE INTERACTIONS

The calculation of the Fermi (contact) hyperfine interaction (Eq.(19)) in the local exchange approximation presents no difficulties when the spin density at the nucleus is the direct contribution of an unpaired electron in an s-type orbital. However, when the spin density at the origin is the result of exchange polarization of s-type orbitals by unpaired p or d electrons, it has been known for some time that the  $X\alpha$  approximation gives poor results, compared to Hartree-Fock<sup>(6)</sup>. An extensive study reported for  $Mn^{+2}$  ion ( $3d^5$ ) indicates that the spin densities at the nucleus of the 1s, 2s and 3s orbitals are systematically smaller than those obtained by the Hartree-Fock method<sup>(27)</sup>. This was ascribed to a slightly larger expansion of the 3d orbital wave functions obtained in the  $X\alpha$  calculation. A systematic study of the  $X\alpha$  spin densities of s shells for the atoms B, N, F, Al, P and Cl (with unpaired p electrons) was reported<sup>(28)</sup>. Values of radial spin densities and spin densities at the origin were compared to spin-polarized Hartree-Fock values. The differences noticed in the radial spin densities are larger near the nucleus than in the valence region. The best agreement found was for B and Al, which may be explained by the fact that the electronic density is more slowly varying for these atoms. A slowly varying density is a condition for the applicability of the statistical  $X\alpha$  approximation.

In spite of these shortcomings, the  $X\alpha$  approximation can still

be made useful in calculations of Fermi hyperfine fields in transition metal compounds. Two cases of Fe complexes were studied<sup>(18)(29)</sup> in detail with the MSX $\alpha$  method, the tetrahedral ions  $\text{FeO}_4^{-2}$  and  $\text{FeS}_4^{-5}$ . The former is known to have two electrons in the last occupied orbital ( $e^2$ ) and a  ${}^3A_2$  ground state<sup>(18)</sup>. The latter is in a high-spin  $3d^5$  configuration, with a  ${}^6A_1$  ground state<sup>(29)</sup>. In both cases, the experimental hyperfine fields are much lower than what would be expected from the spin-polarization due to two ( $\text{FeO}_4^{-2}$ ) and five ( $\text{FeS}_4^{-5}$ ) unpaired electrons in an Fe 3d shell<sup>(6)(30)</sup>. This was ascribed, on the basis of the MSX $\alpha$  calculations, to covalency effects. One of the features noticed is that bonding with the ligands produces an inflow of spin  $\uparrow$  electrons into the Fe(3d) orbital, such that the number of effective unpaired electrons in that orbital is reduced, as compared to the free ions  $\text{Fe}^{+6}$  and  $\text{Fe}^{+3}$ , thus producing a smaller polarization of the inner s shells.

Another study of contact hyperfine terms in an ionic cluster of transition element is the MSX $\alpha$  calculation of  $\text{Co}^{+2}$  in a LiF crystal, represented by the octahedral  $[\text{CoF}_6]^{-4}$  cluster<sup>(31)</sup>. The spin density was calculated both at the  $\text{Co}^{+2}$  and  $\text{F}^-$  nuclei.

An investigation of the spin-Hamiltonian parameters has been performed for  $[\text{CrOCl}_4]^{-1}$ , with wave functions obtained from MSX $\alpha$  calculations<sup>(32)</sup>. The agreement with Electron Spin Resonance data was found to be good. Molecular orbital coefficients, as defined in the MSX $\alpha$  method, and values of  $\langle r^{-3} \rangle_{3d}$ , were needed for the calculations. Similar treatments of the spin hyperfine parameters were given in the theoretical study of ESR spectra of organometallic compounds with the MSX $\alpha$  method. Copper porphine<sup>(33)</sup>

and Cobaltocene  $\text{Cp}_2\text{Co}$  ( $\text{Cp}=\eta^5\text{-cyclopentadienyl}$ )<sup>(34)</sup> are among the organometallics investigated. Several refinements in the method for calculating the hyperfine constants were tested, such as spin-polarization, inclusion of excited states that mix with the ground state via spin-orbit coupling, and use of  $\langle r^{-3} \rangle$  values derived from the molecular functions, instead of atomic Hartree-Fock values.

## V CONCLUSIONS

In analysing the results reviewed here of calculations of hyperfine interactions in transition metal compounds in the local  $X\alpha$  approximation, some conclusions may be extracted. First, it may be observed that, where molecular or cluster calculations are concerned, approximations other than the local exchange have also been employed, such as the muffin-tin potential, or numerical three-dimensional integrations. In this case, it is very difficult to extract from the results the shortcomings which are due solely to the local density approximation. It seems that more systematic investigations would be necessary. Another unfortunate feature is the very small number of "ab-initio" calculations of hyperfine interactions of such systems with which to make comparisons.

Regarding the calculations mentioned here, correlations with experimental results seem to indicate that, as far as trends and qualitative aspects are concerned, the  $X\alpha$  Molecular Orbital methods have led to some understanding of the bonding mechanisms which explain the influence of the different electronic environments on the hyperfine parameters. Much understanding has been gained in this aspect. However, quantitative results at the present



moment seem to be requiring more accurate calculations. Moreover, too little is actually known on the influence of many-body effects which might have an outstanding role in explaining such small interactions.

REFERENCES

1. A. Abragam, "The Principles of Nuclear Magnetism, Oxford University Press, London(1961).
2. B. Bleaney, "Hyperfine Structure and Electron Paramagnetic Resonance", in "Hyperfine Interactions", ed. A. J. Freeman and R. B. Frankel, Academic Press, N.York (1967);  
A. Abragam and B. Bleaney, "Electron Paramagnetic Resonance of Transition Ions", Clarendon Press, Oxford (1970).
3. T. P. Das and E. L. Hahn, "Nuclear Quadrupole Resonance Spectroscopy", Academic Press, N. York(1958).
4. G. M. Bancroft, "Mössbauer Spectroscopy", McGraw-Hill , London (1973);  
N. N. Greenwood and T. C. Gibb, "Mössbauer Spectroscopy", Chapman and Hall, London (1971);  
J. M. Friedt and J. Danon, "Mössbauer Spectroscopy: Principles and Examples of Chemical Applications", in "Modern Physics in Chemistry ", vol.2, ed. E. Fluck and V. I. Goldanskii, Academic Press, London (1979)
5. R. D. Gill, "Gamma-ray Angular Correlations", Academic Press, N. York (1975);  
H. Frauenfelder and R. M. Steffen, in "Alpha-Beta - and Gamma-ray Spectroscopy", vol,2, ed. K. Siegbahn, North-Holland, Amsterdam (1965).
6. J. C. Slater, "The Self-consistent Field for Molecules and Solids", vol.4 of "Quantum Theory of Molecules and Solids", McGraw-Hill, N. York (1974).
7. B. D. Dunlap and G. M. Kalvius, "Theory of Isomer Shifts",

- in "Mössbauer Isomer Shifts", ed. G. K. Shenoy and F. E. Wagner, North-Holland, Amsterdam (1978).
8. E. N. Kaufmann and R. J. Vianden, Rev. Mod. Phys., 51, 161 (1979), and references therein.
  9. R. E. Watson and A. J. Freeman, "Hartree-Fock Theory of Electric and Magnetic Hyperfine Interactions in Atoms and Magnetic Compounds", in "Hyperfine Interactions", ed. A. J. Freeman and R. B. Frankel, Academic Press, New York (1967).
  10. W. Kohn and L. J. Sham, Phys. Rev.A, 140, 1133 (1965).
  11. J. C. Slater and K. H. Johnson, Phys. Rev.B, 5, 844(1972); J. C. Slater, Advan. Quant. Chem., 6, 1(1972); K. J. Johnson, Advan. Quant. Chem, 7, 143 (1973).
  12. D. E. Ellis, Int. J. Quant. Chem, S2, 35(1968); D. E. Ellis and G. S. Painter, Phys. Rev.B, 2, 2887 (1970); A. Rosén, D. E. Ellis, H. Adachi and F. W. Averill, J. Chem. Phys., 85, 3629 (1976).
  13. P. F. Walch and D. E. Ellis, Phys. Rev.B, 7, 903(1973).
  14. D. E. Ellis and F. W. Averill, J. Chem. Phys., 60, 2856 (1974).
  15. M. L. de Siqueira, S. Larsson and J. W. D. Connolly, J. Phys. Chem. Solids, 36, 1419 (1975).
  16. D. Guenzburger, B. Maffeo and M. L. de Siqueira, J. Phys. Chem. Solids, 38, 35 (1977).
  17. D. Guenzburger, B. Maffeo and S. Larsson, Int. J. Quant. Chem., 12, 383 (1977).
  18. D. Guenzburger, D. M. S. Esquivel and J. Danon, Phys. Rev.B.,18, 4561 (1978).

19. S. Larsson, Theoret. Chim. Acta, 49, 45(1978) .
20. W. C. Nieuwpoort, D. Post and P. Th. Van Duijnen, Phys. Rev.B, 17, 91(1978) .
21. D. Guenzburger and E. M. B. Saitovitch, Phys.Rev.B, 24, 2368(1981).
22. D. Guenzburger, E. M. B. Saitovitch, M. A. de Paoli and H. Manela, to be submitted for publication.
23. M. A. de Paoli, E. M. B. Saitovitch, S.Oliveira and D. Guenzburger, to be submitted for publication.
24. S. K. Lie, D. M. S. Esquivel and D. Guenzburger, Chem. Phys. Letters, 57, 458(1978).
25. M. Braga, A. C. Pavão and J. R. Leite, Phys. Rev.B, 23, 4328(1981).
26. D. Guenzburger and D. E. Ellis, Phys. Rev.B, 22, 4203(1980).
27. T. M. Wilson, J. H. Wood and J. C. Slater , Phys . Rev.A, 2, 620(1970).
28. R. Ahlberg and S. Larsson, Chem. Phys. Letters, 49, 491(1977).
29. C. A. Taft and M. Braga, Phys. Rev.B, 21, 5802 (1980).
30. R. E. Watson and A. J. Freeman, Phys. Rev., 123, 2027(1961).
31. E. L. Albuquerque, B. Maffeo, H. S. Brandi and M. L. de Siqueira, Solid State Comm., 18, 1381(1976).

32. K. K. Sunil, J. F. Harrison and M. T. Rogers, J. Chem. Phys., 76, 3078(1982).
33. D. A. Case and M. Karplus, J. Am. Chem. Soc., 99, 6182(1977).
34. J. Weber, A. Goursot, E. Pénigault, J. H. Ammeter and J. Bachmann, J. Am. Chem. Soc., 104, 1491 (1982).

TABLE CAPTIONS

TABLE I

Values of  $|\Psi(0)|^2$  in  $a_0^{-3}$  (1s and 2s electrons excluded) calculated with the MSX $\alpha$  method for various complexes of Fe. Fluorine anions from Ref. (15),  $[\text{Fe}(\text{CN})_6]^{-4}$  from Ref. (16),  $[\text{Fe}(\text{CN})_6]^{-3}$  from Ref. (17), and  $\text{FeO}_4^{-2}$  from Ref. (18).

TABLE II

Values of  $|\Psi(0)|^2$  in  $a_0^{-3}$ , experimental and calculated isomer shifts and quadrupole splittings, and Fe populations for  $\text{Fe}(\text{CO})_5$  and  $\text{Fe}(\text{CO})_4$ . The IS for  $\text{Fe}(\text{CO})_4$  was calculated by fitting the experimental value of the IS for  $\text{Fe}(\text{CO})_5$ , and using  $\alpha = -0.29$ .  $\Delta\text{EQ}$  for  $\text{Fe}(\text{CO})_4$  was obtained with  $Q(\text{Fe}) = 0.158$  barn, which reproduces the experimental  $\Delta\text{EQ}$  of  $\text{Fe}(\text{CO})_5$ . The IS values are referred to Fe metal.

FIGURE CAPTIONS

FIGURE I

Values of  $|\Psi(0)|^2$  calculated with the MSX $\alpha$  method (1s and 2s orbitals excluded), plotted against isomer shifts of  $^{57}\text{Fe}$ . See Refs. (15)-(18) for details of calculations and references to isomer shifts values. The two values of  $|\Psi(0)|^2$  for  $\text{FeF}_6^{-4}$  and  $\text{FeF}_6^{-3}$  refer to two different muffin-tin radii.

FIGURE II

Values of  $|\Psi(0)|^2$  (1s and 2s orbitals excluded) at an Fe nucleus of  $\text{Fe}_2$ , at different interatomic distances, for configuration  $(\dots 1\delta_g^2 1\delta_u^2 6\sigma_u^2 3\pi_g^2)$

TABLE I

	$\text{FeF}_6^{-3}$		$\text{FeF}_6^{-4}$		$\text{FeF}_6^{-5}$	$[\text{Fe}(\text{CN})_6]^{-4}$	$[\text{Fe}(\text{CN})_6]^{-3}$	$\text{FeO}_4^{-2}$
	$R_{\text{Fe}}=1.76 \text{ a.u.}$ $\text{Fe-F}=1.80\text{\AA}$	$R_{\text{Fe}}=1.76 \text{ a.u.}$ $\text{Fe-F}=1.91\text{\AA}$	$R_{\text{Fe}}=2.04 \text{ a.u.}$ $\text{Fe-F}=2.06\text{\AA}$	$R_{\text{Fe}}=1.76 \text{ a.u.}$ $\text{Fe-F}=2.06\text{\AA}$	$R_{\text{Fe}}=1.76 \text{ a.u.}$ $\text{Fe-F}=2.18\text{\AA}$	$R_{\text{Fe}}=2.48 \text{ a.u.}$ $\text{Fe-C}=1.92\text{\AA}$	$R_{\text{Fe}}=2.47 \text{ a.u.}$ $\text{Fe-C}=1.90\text{\AA}$	$R_{\text{Fe}}=2.00 \text{ a.u.}$ $\text{Fe-O}=1.65\text{\AA}$
3s	140.25	140.58	140.22	139.63	138.73	140.45	140.51	141.17
Valence	4.12	3.07	2.51	1.94	1.30	6.40	6.94	7.49
Total	144.37	143.65	142.73	141.57	140.03	146.85	147.45	148.66



TABLE II

Fe(CO) <sub>5</sub> D <sub>3h</sub>		Fe(CO) <sub>4</sub> C <sub>2v</sub>	
8a <sub>1</sub> (3s)	140.46	7a <sub>1</sub> ' (3s)	140.41
9a <sub>1</sub> -19a <sub>1</sub>	<u>6.99</u>	8a <sub>1</sub> '-13a <sub>1</sub> '	<u>6.63</u>
Total	147.45	Total	147.04
3d population:	6.65	3d population:	6.61
4s population:	0.01	4s population:	0.07
IS measured: -0.174±0.005		IS measured: -0.124±0.008	
IS calculated: -0.174		IS calculated: - 0.060	
	(mm/s)		(mm/s)
ΔEQ measured: +2.52±0.01		ΔEQ measured: 1.83±0.02	
ΔEQ calculated: +2.52		ΔEQ calculated: +1.62	
	(mm/s)		(mm/s)

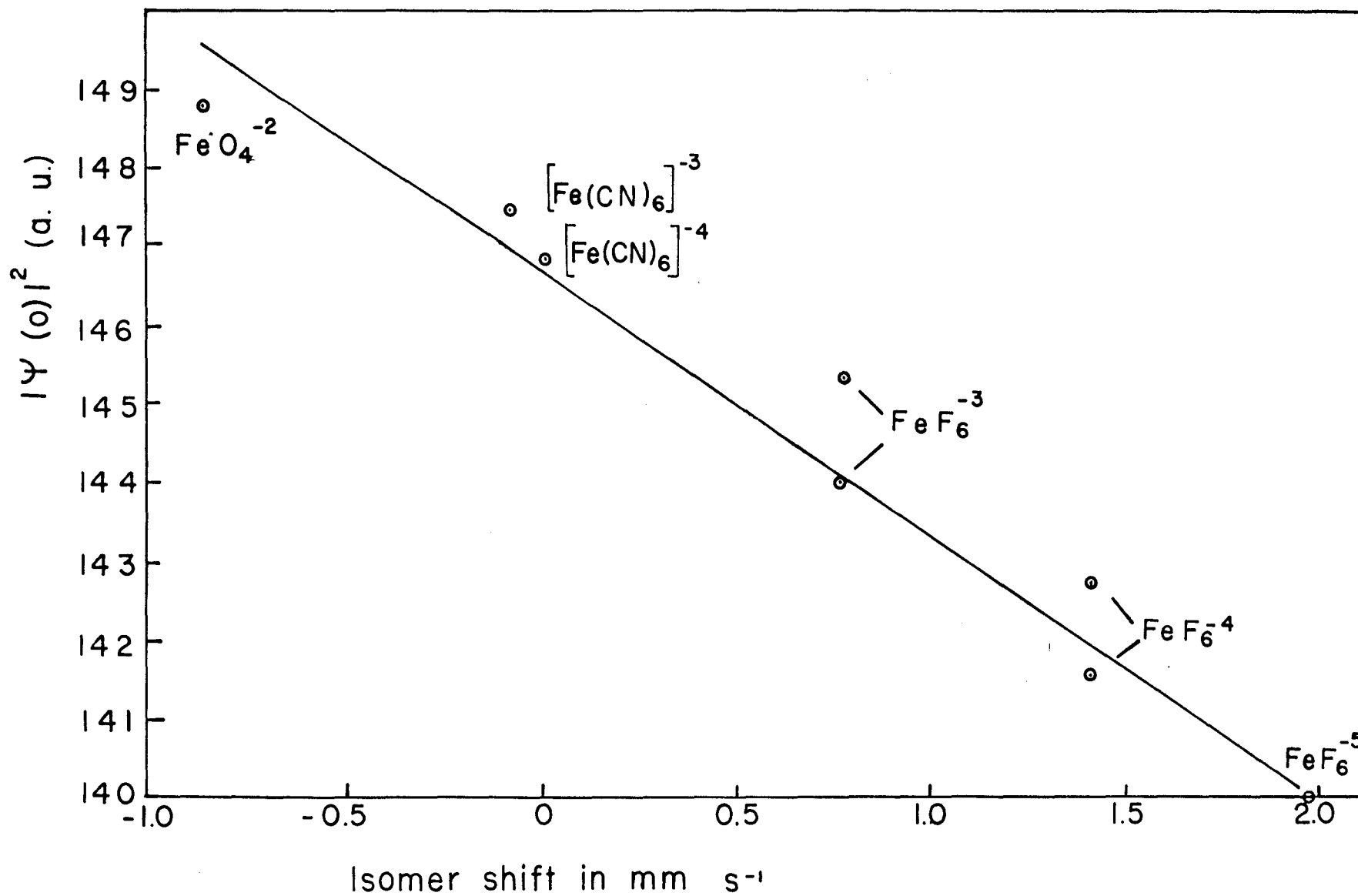


FIG. 1

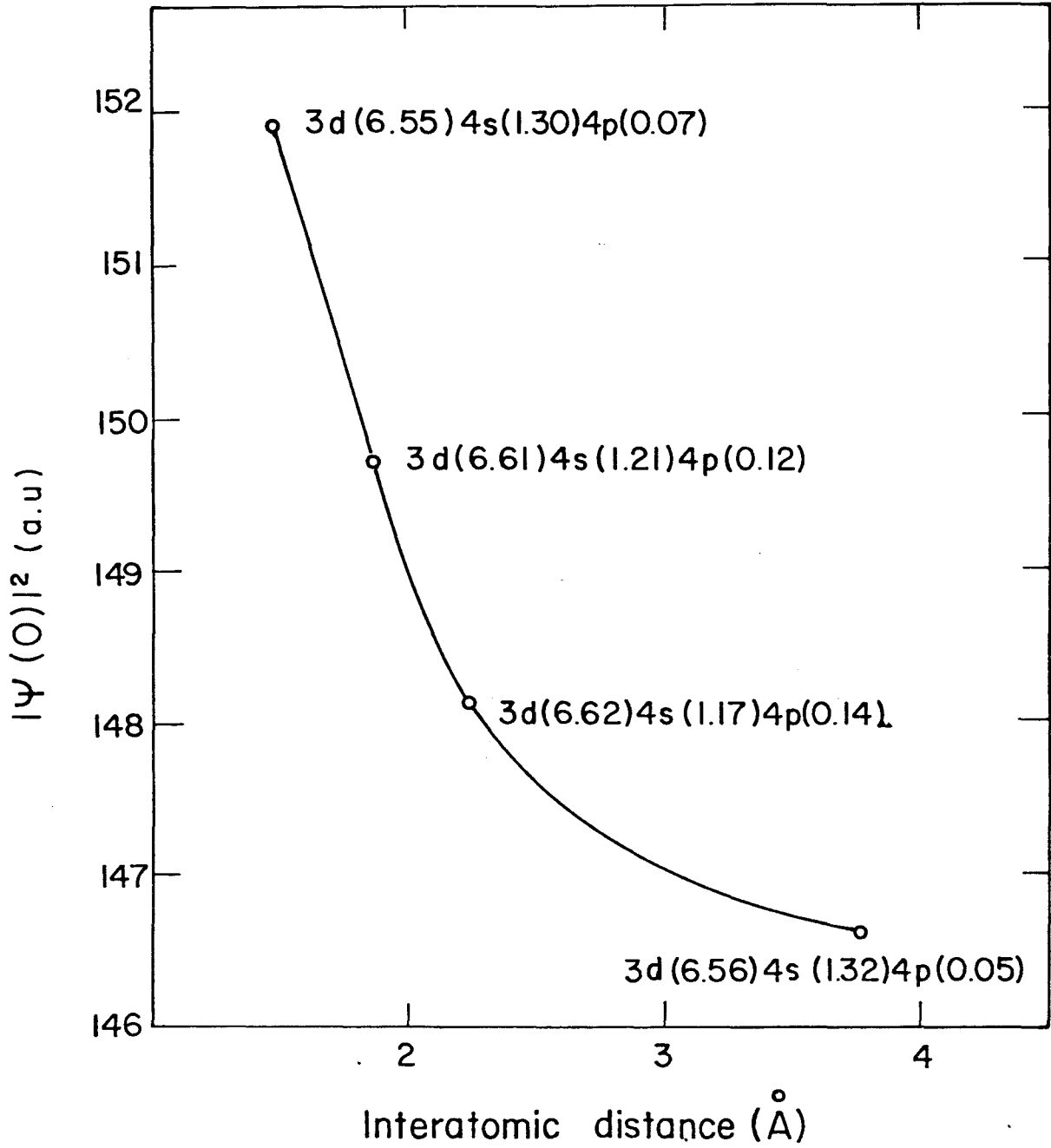


FIG. II